



Closing a gap in tropical forest biomass estimation: taking crown mass variation into account in pantropical allometries

Pierre Ploton^{1,2}, Nicolas Barbier¹, Stéphane Takoudjou Momo^{1,3}, Maxime Réjou-Méchain^{1,4,5}, Faustin Boyemba Bosela⁶, Georges Chuyong⁷, Gilles Dauby^{8,9}, Vincent Droissart^{1,10}, Adeline Fayolle¹¹, Rosa Calisto Goodman¹², Matieu Henry¹³, Narcisse Guy Kamdem³, John Katembo Mukirania⁶, David Kenfack¹⁴, Moses Libalah³, Alfred Ngomanda¹⁵, Vivien Rossi^{4,16}, Bonaventure Sonké³, Nicolas Texier^{1,3}, Duncan Thomas¹⁷, Donatien Zebaze³, Pierre Couteron¹, Uta Berger¹⁸, and Raphaël Pélissier¹

¹Institut de Recherche pour le Développement, UMR-AMAP, Montpellier, France

²Institut des sciences et industries du vivant et de l'environnement, Montpellier, France

³Laboratoire de Botanique systématique et d'Ecologie, Département des Sciences Biologiques, Ecole Normale Supérieure, Université de Yaoundé I, Yaoundé, Cameroon

⁴Centre de coopération internationale en recherche agronomique pour le développement, Montpellier, France

⁵Geomatics and Applied Informatics Laboratory (LIAG), French Institute of Pondicherry, Puducherry, India

⁶Faculté des Sciences, Université de Kisangani, Kisangani, Democratic Republic of Congo

⁷Department of Botany and Plant Physiology, University of Buea, Buea, Cameroon

⁸Institut de Recherche pour le Développement, UMR-DIADE, Montpellier, France

⁹Evolutionary Biology and Ecology, Faculté des Sciences, Université Libre de Bruxelles, Brussels, Belgium

¹⁰Herbarium et Bibliothèque de Botanique africaine, Université Libre de Bruxelles, Brussels, Belgium

¹¹Research axis on Forest Resource Management of the Biosystem engineering (BIOSE), Gembloux Agro-Bio Tech, Université de Liège, Gembloux, Belgium

¹²Yale School of Forestry and Environmental Studies, New Haven, USA

¹³Food and Agriculture Organization of the United Nations, Rome, Italy

¹⁴Center for Tropical Forest Science, Harvard University, Cambridge, USA

¹⁵Institut de Recherche en Ecologie Tropicale, Libreville, Gabon

¹⁶Département d'Informatique, Université de Yaoundé I, UMMISCO, Yaoundé, Cameroon

¹⁷Department of Botany and Plant Pathology, Oregon State University, Corvallis, USA

¹⁸Technische Universität Dresden, Faculty of Environmental Sciences, Institute of Forest Growth and Forest Computer Sciences, Tharandt, Germany

Correspondence to: Pierre Ploton (pierre.ploton@ird.fr)

Received: 17 October 2015 – Published in Biogeosciences Discuss.: 10 December 2015

Revised: 22 February 2016 – Accepted: 29 February 2016 – Published: 14 March 2016

Abstract. Accurately monitoring tropical forest carbon stocks is a challenge that remains outstanding. Allometric models that consider tree diameter, height and wood density as predictors are currently used in most tropical forest carbon studies. In particular, a pantropical biomass model has been widely used for approximately a decade, and its most recent version will certainly constitute a reference model in the coming years. However, this reference model shows a systematic bias towards the largest trees. Because large trees

are key drivers of forest carbon stocks and dynamics, understanding the origin and the consequences of this bias is of utmost concern. In this study, we compiled a unique tree mass data set of 673 trees destructively sampled in five tropical countries (101 trees > 100 cm in diameter) and an original data set of 130 forest plots (1 ha) from central Africa to quantify the prediction error of biomass allometric models at the individual and plot levels when explicitly taking crown mass variations into account or not doing so. We first showed that

the proportion of crown to total tree aboveground biomass is highly variable among trees, ranging from 3 to 88 %. This proportion was constant on average for trees < 10 Mg (mean of 34 %) but, above this threshold, increased sharply with tree mass and exceeded 50 % on average for trees ≥ 45 Mg. This increase coincided with a progressive deviation between the pantropical biomass model estimations and actual tree mass. Taking a crown mass proxy into account in a newly developed model consistently removed the bias observed for large trees (> 1 Mg) and reduced the range of plot-level error (in %) from [−23; 16] to [0; 10]. The disproportionally higher allocation of large trees to crown mass may thus explain the bias observed recently in the reference pantropical model. This bias leads to far-from-negligible, but often overlooked, systematic errors at the plot level and may be easily corrected by taking a crown mass proxy for the largest trees in a stand into account, thus suggesting that the accuracy of forest carbon estimates can be significantly improved at a minimal cost.

1 Introduction

Monitoring forest carbon variation in space and time is both a sociopolitical challenge for climate change mitigation and a scientific challenge, especially in tropical forests, which play a major role in the global carbon balance (Hansen et al., 2013; Harris et al., 2012; Saatchi et al., 2011). Significant milestones have been reached in the last decade thanks to the development of broad-scale remote sensing approaches (Baccini et al., 2012; Malhi et al., 2006; Mitchard et al., 2013; Saatchi et al., 2011). However, local forest biomass estimations commonly represent the foundation for the calibration and validation of remote sensing models. As a consequence, uncertainties and errors in local biomass estimations may propagate dramatically to broad-scale forest carbon stock assessment (Avitabile et al., 2011; Pelletier et al., 2011; Réjou-Méchain et al., 2014). Aboveground biomass (AGB) is the major pool of biomass in tropical forests (Eggleston et al., 2006). The AGB of a tree (or TAGB) is generally predicted by empirically derived allometric equations that use measurements of the size of an individual tree as predictors of its mass (Clark and Kellner, 2012). Among these predictors, diameter at breast height (D) and total tree height (H) are often used to capture volume variations between trees, whereas wood density (ρ) is used to convert volume to dry mass (Brown et al., 1989). The most frequently used allometric equations for tropical forests (Chave et al., 2005, 2014) have the following form: $\text{TAGB} = \alpha \times (D^2 \times H \times \rho)^\beta$, where diameter, height and wood density are combined into a single compound variable related to dry mass through a power law of parameters α and β . This model form, referred to hereafter as our reference allometric model form, performs well when $\beta = 1$ or close to 1 (Chave et al., 2005, 2014), meaning that trees can roughly be viewed as a standard geometric solid for

which the parameter α determines the shape (or form factor) of the geometric approximation. However, the uncertainty associated with this model is still very high, with an average error of 50 % at the tree level, illustrating the high natural variability of mass between trees with similar D , H and ρ values. More importantly, this reference allometric model shows a systematic underestimation of TAGB of approximately 20 % on average for the heaviest trees (> 30 Mg; Fig. 2 in Chave et al., 2014), which may contribute strongly to uncertainty in biomass estimates at the plot level. It is often argued that, by definition, the least-squares regression model implies that tree-level errors are globally centered on 0, thus limiting the plot-level prediction error to approximately 5–10 % for a standard 1 ha forest plot (Chave et al., 2014; Moundounga Mavouroulou et al., 2014). However, systematic errors associated with large trees are expected to disproportionally propagate to plot-level predictions because of their prominent contribution to plot AGB (Bastin et al., 2015; Clark and Clark, 1996; Sist et al., 2014; Slik et al., 2013; Stephenson et al., 2014). Thus, identifying the origin of systematic errors in such biomass allometric models is a prerequisite for improving local biomass estimations and thus limiting the risk of uncontrolled error propagation to broad-scale extrapolations.

As foresters have known for decades, it is reasonable to approximate stem volume using a geometric shape. Such an approximation, however, is questionable for assessing the total tree volume, including the crown. Because β is generally close to 1 in the reference allometric model, the relative proportion of crown to total tree mass (or crown mass ratio) directly affects the adjustment of the tree form factor α (e.g., Cannell, 1984). Moreover, the crown mass ratio is known to vary greatly between species, reflecting different strategies of carbon allocation. For instance, Cannell (1984) observed that coniferous species have a lower proportion of crown mass (10–20 %) than tropical broadleaved species (over 35 %), whereas temperate softwood species were found to have a lower and less variable crown mass ratio (20–30 %) than temperate hardwood species (20–70 %; Freedman et al., 1982; Jenkins et al., 2003). In the tropics, distinct crown size allometries have been documented among species functional groups (Poorter et al., 2003, 2006; Van Gelder et al., 2006). For instance, at comparable stem diameters, pioneer species tend to be taller and to have shorter and narrower crowns than understory species (Poorter et al., 2006). These differences reflect strategies of energy investment (tree height vs. crown development) are likely to result in different crown mass ratios among trees with similar D^2 , H and ρ values. Indeed, Goodman et al. (2014) obtained a substantially improved biomass allometric model when crown diameter was incorporated into the equation to take individual variation in crown size into account.

Destructive data on tropical trees featuring information on both crown mass and classical biometric measurements (D , H , ρ) are scarce and theoretical work on crown properties largely remains to be validated with field data. In most empir-

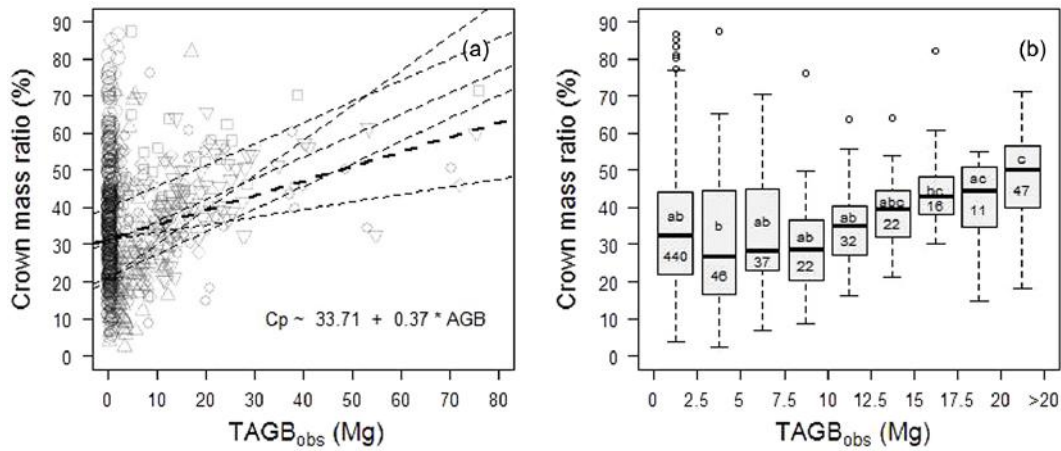


Figure 1. Panel (a): distribution of crown mass ratio (in %) along the range of tree mass ($TAGB_{obs}$, in Mg) for 673 trees. Dashed lines represent the fit of robust regressions (model II linear regression fitted using ordinary least square) performed on the full crown mass data set (thick line; one-tailed permutation test on slope: p value < 0.001) and on each separate source (thin lines), with symbols indicating the source as follows: empty circles from Vieilledent et al. (2011); regression line not represented since the largest tree is 3.7 Mg only); solid circles from Fayolle et al. (2013); squares from Goodman et al. (2013, 2014); diamonds from Henry et al. (2010); head-up triangles from Ngomanda et al. (2014); and head-down triangles from the unpublished data set from Cameroon. Panel (b): variation in crown mass ratio (in %) across tree mass bins of equal width (2.5 Mg). The last bin contains all trees ≥ 20 Mg. The number of individuals per bin and the results of nonparametric pairwise comparisons are represented below and above the median lines, respectively.

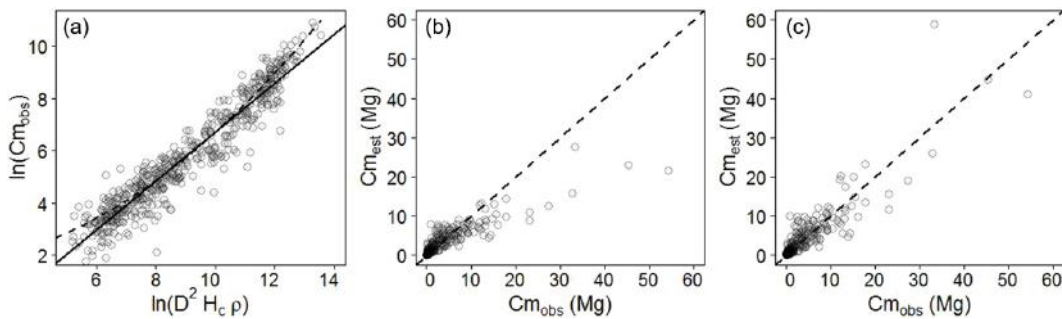


Figure 2. Panel (a): observed crown mass vs. the compound variable $D^2 \times Hc \times \rho$ (in log scale), displaying a slightly concave relationship. The crown mass sub-model sm_1 does not capture this effect (model fit represented with a full line in a), resulting in biased model predictions (b), whereas sub-model sm_3 does not present this error pattern (model fit represented as a dashed line in (a); observed crown mass against model predictions in c). Models were fitted to $Data_{CM2}$ (crown mass database).

ical studies published to date, crown mass models use trunk diameter as a single predictor (see, e.g., Nogueira et al., 2008, and Chambers et al., 2001). Such models often provide good results ($R^2 \geq 0.9$), which reflect the strong biophysical constraints exerted by the diameter of the first pipe (the trunk) on the volume of the branching network (Shinozaki et al., 1964). However, theoretical results suggest that several crown metrics would scale with crown mass. For instance, Mäkelä and Valentine (2006) modified the allometric scaling theory (Enquist, 2002; West et al., 1999) by incorporating self-pruning processes into the crown. The authors showed that crown mass is expected to be a power function of the total length of the branching network, which they approximated by crown depth (i.e., total tree height minus trunk height). The construction of the crown and its structural properties have also

largely been studied in the light of the mechanical stresses faced by trees (such as gravity and wind; see, e.g., McMahon and Kronauer, 1976; Eloy, 2011). Within this theoretical frame, crown mass can also be expressed as a power function of crown diameter (King and Loucks, 1978).

In the present study, we used a unique tree mass data set containing crown mass information on 673 trees from five tropical countries and a network of forest plots covering 130 ha in central Africa to (i) quantify the variation in crown mass ratio in tropical trees; (ii) assess the contribution of crown mass variation to the reference pantropical model error, either at the tree level or when propagated to the plot level; and (iii) propose a new operational strategy to explicitly take crown mass variation into account in biomass allometric equations. We hypothesize that the variation in the

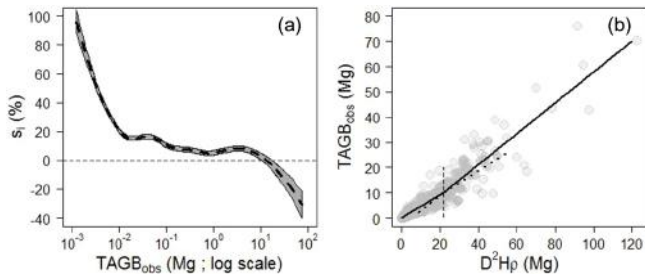


Figure 3. Panel (a): relative individual residuals (s_i in %) of the reference biomass allometric pantropical model of Chave et al. (2014) against the tree AGB gradient. The thick dashed line represents the fit of a local regression (loess function, span=0.5) bounded by standard errors. Panel (b): observed tree AGB (TAGB_{obs}) vs. the compound variable $D^2 \times H \times \rho$, with D and H being the tree stem diameter and height, respectively, and ρ the wood density. A segmented regression revealed a significant break point (thin vertical dashed line) at approximately 10 Mg of TAGB_{obs} (Davies test p value $< 2.2 \times 10^{-16}$).

crown mass ratio in tropical trees is a major source of error in current biomass allometric models and that taking this variation into account would significantly reduce uncertainty associated with plot-level biomass predictions.

2 Materials and methods

2.1 Biomass data

We compiled tree AGB data from published and unpublished sources providing information on crown mass for 673 tropical trees belonging to 132 genera (144 identified species), with a wide tree size range (i.e., diameter at breast height, D : 10–212 cm) and aboveground tree masses of up to 76 Mg. An unpublished data set for 77 large trees (with $D \geq 67$ cm) was obtained from the fieldwork of Pierre Ploton, Nicolas Barbier and Stéphane Takoujdou Momo in semi-deciduous forests of eastern Cameroon (site characteristics and field protocol in Supplement Sects. S1.1 and S1.2.1). The remaining data sets were gathered from relevant published studies: 29 trees from Ghana (Henry et al., 2010), 285 trees from Madagascar (Vieilledent et al., 2011), 51 trees from Peru (Goodman et al., 2014, 2013), 132 trees from Cameroon (Fayolle et al., 2013) and 99 trees from Gabon (Ngomanda et al., 2014). The whole data set is available from the Dryad Data Repository (<http://dx.doi.org/10.5061/dryad.f2b52>), with details about the protocol used to integrate data from published studies presented in the Supplement (Sect. S1.2.2). For the purpose of some analyses, we extracted from this crown mass database (hereafter referred to as Data_{CM1}) a subset of 541 trees for which total tree height was available (Data_{CM2} ; all but Fayolle et al., 2013) and another subset of 119 trees for which crown diameter was also available (Data_{CD} ; all but Vieilledent et al., 2011; Fayolle et al., 2013; Ngomanda et

al., 2014; and 38 trees from our unpublished data set). Finally, we used as a reference the data from Chave et al. (2014) on the total mass (but not crown mass) of 4004 destructively sampled trees of many different species from all around the tropical world (Data_{REF}).

2.2 Forest inventory data

We used a set of 81 large forest plots (> 1 ha), covering a total area of 130 ha, to propagate TAGB estimation errors to plot-level predictions. The forest inventory data contained the taxonomic identification of all trees with a diameter at breast height ($D \geq 10$ cm), as well as total tree height measurements (H) for a subset of trees, from which we established plot-level H vs. D relationships to predict the height of the remaining trees. Details about the inventory protocol along with statistical procedures used to compute plot AGB (or PAGB) from field measurements are provided in the Supplement (Sect. S1.3). Among these plots, 80 were from a network of 1 ha plots established in humid evergreen to semi-deciduous forests belonging to 13 sites in Cameroon, Gabon and the Democratic Republic of Congo (unpublished data)¹. In addition, we included a 50 ha permanent plot from Korup National Park, in the evergreen Atlantic forest of western Cameroon (Chuyong et al., 2004), which we subdivided into 1 ha subplots. Overall, the inventory data encompassed a high diversity of stand structural profiles ranging from open-canopy *Marantaceae* forests to old-growth monodominant *Gilbertiodendron dewevrei* stands and including mixed *terra firme* forests with various levels of degradation.

2.3 Allometric model fitting

We fitted the pantropical allometric model of Chave et al. (2014) to log-transformed data using ordinary least-squares regression:

$$\ln(\text{TAGB}) = \alpha + \beta \times \ln(D^2 \times H \times \rho) + \varepsilon, \quad (1)$$

with TAGB (in kg) representing the aboveground tree mass, D (in cm) the tree stem diameter, H (in m) the total tree height, ρ (in g cm^{-3}) the wood density and ε the error term, which is assumed to follow a normal distribution $N(0, \text{RSE}^2)$, where RSE is the residual standard error of the model. This model, denoted by m_0 , was considered as the reference model.

To assess the sensitivity of m_0 to crown mass variations, we built a model (m_1) that restricted the volume approximation to the trunk compartment and included actual crown mass as an additional covariate:

$$\ln(\text{TAGB}) = \alpha + \beta \times \ln(D^2 \times \text{Ht} \times \rho) + \gamma \times \ln(\text{Cm}) + \varepsilon, \quad (2)$$

¹Metadata available at <http://vmamapgn-test.mpl.ird.fr:8080/geonetwork/srv/eng/search#7dd46c7d-db2f-4bb0-920a-8afe4832f1b3>.

with C_m representing the crown mass (in kg) and H_t the trunk height (i.e., height of the first main branch; in m). Note that model m_1 cannot be operationally implemented (which would require destructive measurements of crowns) but quantifies the maximal improvement that can be made through the inclusion of crown mass proxies in a biomass allometric model.

2.4 Development of crown mass proxies

We further developed crown mass proxies to be incorporated in place of the real crown mass (C_m) in the allometric model m_1 . From preliminary tests of various model forms (see Appendix A), we selected a crown mass sub-model based on a volume approximation similar to that made for the trunk component (sm_1):

$$\ln(C_m) = \alpha + \beta \times \ln(D^2 \times H_c \times \rho) + \varepsilon, \quad (3)$$

where D is the trunk diameter at breast height (in cm) and H_c the crown depth (that is, $H - H_t$; in m), available in our data set $Data_{CM2}$ ($n = 541$).

In this sub-model, tree crowns of short height but large width are assigned a small H_c and thus a small mass, whereas the volume they occupy is more horizontal than vertical. We thus tested in sub-model sm_2 (Eq. 4) whether using the mean crown size (Eq. 5), which takes both H_c and C_d (the crown diameter in meters available in our data set $Data_{CD}$; $n = 119$) into account, reduces the error associated with sm_1 :

$$\ln(C_m) = \alpha + \beta \times \ln(D^2 \times C_s \times \rho) + \varepsilon \quad (4)$$

$$C_s = \frac{(H_c + C_d)}{2}. \quad (5)$$

Finally, Sillett et al. (2010) showed that for large, old trees, a temporal increment of D and H poorly reflects the high rate of mass accumulation within crowns. We thus hypothesized that the relationship between C_m and $D^2 \times H_c \times \rho$ (or $D^2 \times C_s \times \rho$) depends on tree size and fitted a quadratic (second-order) polynomial model to take this phenomenon into account (Niklas, 1995):

$$\ln(C_m) = \alpha + \beta \times \ln(D^2 \times H_c \times \rho) + \gamma \times \ln(D^2 \times H_c \times \rho)^2 + \varepsilon \quad (6)$$

$$\ln(C_m) = \alpha + \beta \times \ln(D^2 \times C_s \times \rho) + \gamma \times \ln(D^2 \times C_s \times \rho)^2 + \varepsilon, \quad (7)$$

where Eqs. (6) and (7) are referred to as sub-models sm_3 and sm_4 , respectively.

2.5 Model error evaluation

2.5.1 Tree level

From biomass allometric equations, we estimated crown mass (denoted by $C_{m_{est}}$) or total tree aboveground mass (denoted by $TAGB_{est}$) including Baskerville (1972) bias correction during back-transformation from the logarithmic scale to

the original mass unit (i.e., kg). In addition to classical criteria of model fit assessment (adjusted R^2 , residual standard error, Akaike information criterion), we quantified model uncertainty based on the distribution of individual relative residuals (in %), which is defined as follows:

$$s_i = \left(\frac{Y_{est,i} - Y_{obs,i}}{Y_{obs,i}} \right) \times 100, \quad (8)$$

where $Y_{obs,i}$ and $Y_{est,i}$ are the crown or tree biomass values in the calibration data set (i.e., measured in the field) and those allometrically estimated for tree i , respectively. We reported the median of $|s_i|$ values, hereafter referred to as “ S ”, as an indicator of model precision. For a tree biomass allometric model to be unbiased, we expect s_i to be locally centered on zero for any given small range of the tree mass gradient. We thus investigated the distribution of s_i values with respect to tree mass using local regression (loess method; Cleveland et al., 1992).

2.5.2 Plot level

Allometric models are mostly used to make plot-level AGB predictions from nondestructive forest inventory data. Such plot-level predictions are obtained by simply summing individual predictions over all trees in a plot ($PAGB_{pred} = \sum_i TAGB_{pred}$). Prediction errors at the tree level are thus expected to yield an error at the plot level, which may depend on the actual tree mass distribution in the sample plot. To take this effect into account, we developed a simulation procedure, implemented in two steps, which propagated $TAGB_{pred}$ errors to $PAGB_{pred}$. The first step consists of attributing to each tree i in a given plot a value of $TAGB_{sim}$ corresponding to the actual AGB of a similar felled tree selected in $Data_{REF}$ based on its nearest neighbor in the space of the centered-reduced variables D , H and ρ (here taken as species average from Dryad Global Wood Density Database; Chave et al., 2009; Zanne et al., 2009). In a second step, the simulation propagates individual errors of a given allometric model using the local distribution of s_i values as predicted by the loess regression: for each $TAGB_{sim}$, we drew a s_{sim} value from a local normal distribution fitted with the loess parameters (i.e., local mean and standard deviation) predicted for that particular $TAGB_{sim}$. Thus, we generated for each 1 ha plot a realistic $PAGB_{sim}$ (i.e., based on observed felled trees) with repeated realizations of a plot-level prediction error (in %) computed for n trees as follows:

$$S_{plot} = \frac{\sum_{i=1}^n (s_{sim}(i) \times TAGB_{sim}(i))}{\sum_{i=1}^n TAGB_{sim}(i)}. \quad (9)$$

For each of the simulated plots, we provided the mean and standard deviation of 1000 realizations of the plot-level prediction error.

All analyses were performed with R statistical software 2.15.2 (R Core Team, 2012), using packages `lmodel2` (Leg-

endre, 2011), segmented (Muggeo, 2003), FNN (Beygelzimer et al., 2013) and msir (Scrucca, 2011).

3 Results

3.1 Contribution of crown to tree mass

Our crown mass database (Data_{CM1}; 673 trees, including 128 trees >10 Mg) revealed a huge variation in the contribution of crown to total tree mass, ranging from 2.5 to 87.5 % of total aboveground biomass, with a mean of 35.6 % ($\pm 16.2\%$). Despite this variation, a linear regression (model II) revealed a significant increase in the crown mass ratio with tree mass of approximately 3.7 % per 10 Mg (Fig. 1a). A similar trend was observed at every site, except for the Ghana data set (Henry et al., 2010), for which the largest sampled tree (72 Mg) had a rather low crown mass ratio (46 %). Overall, this trend appeared to have been driven by the largest trees in the database (Fig. 1b). Indeed, the crown mass ratio appeared to be nearly constant for trees ≤ 10 Mg with an average of 34.0 % ($\pm 16.9\%$) and then to increase progressively with tree mass, exceeding 50 % on average for trees ≥ 45 Mg.

3.2 Crown mass sub-models

All crown mass sub-models provided good fits with our data ($R^2 \geq 0.9$; see Table 1). However, when information on crown diameter was available (Data_{CD}), models that included mean crown size in the compound variable (i.e., Cs, a combination of crown depth and diameter, in sm₂ and sm₄) gave lower AICs and errors (RSE and S) than models that included the simpler crown depth metric (i.e., Hc in sm₁ and sm₃). The quadratic model form provided a better fit than the linear model form (e.g., sm₃ vs. sm₁ fitted to Data_{CM2}), which can be explained by the nonlinear increase in crown mass with either of the two proxy variables ($D^2 \times Hc \times \rho$ or $D^2 \times Cs \times \rho$). The slope of the relationship between crown mass and, for example, $D^2 \times Hc \times \rho$ presented a breaking point at approximately 7.5 Mg (Davies test $P < 0.001$) that was not captured by sub-model sm₁ (Fig. 2a, full line), leading to a substantial bias in back-transformed crown mass estimations (approximately 50 % of observed crown mass for Cm_{obs} ≥ 10 Mg, Fig. 2b). The quadratic sub-model sm₃ provided fairly unbiased crown mass estimations (Fig. 2c). Because the first-order term was never significant in the quadratic sub-models, we retained only the second-order term as a crown mass proxy in the biomass allometric models (see below).

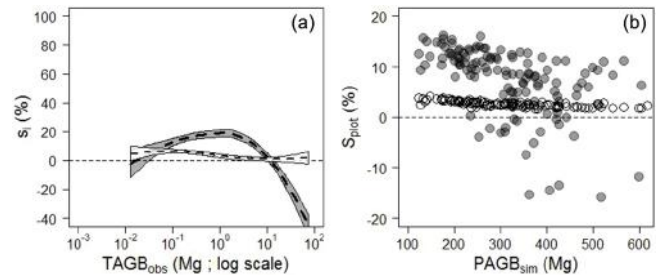


Figure 4. Panel (a): relative residuals (s_i , in %) of the reference biomass allometric model m_0 (grey background) and our model m_1 including crown mass (white background). Thick dashed lines represent fits of local regressions (loess function; span: 1) bounded by standard errors. Panel (b): propagation of individual estimation errors of m_0 (solid grey circles) and m_1 (empty circles) to the plot level.

3.3 Taking crown mass into account in biomass allometric models

The reference model (m_0) proposed by Chave et al. (2014) presented, when fitted to DATA_{REF}, a bias that was a function of tree mass, with a systematic AGB overestimation for trees smaller than approximately 10 Mg and an underestimation for larger trees, reaching approximately 25 % for trees greater than 30 Mg (Fig. 3a). This bias pattern reflected a breaking point in the relationship between $D^2 \times H \times \rho$ and TAGB_{obs} (Davies test $P < 0.001$) located at approximately 10 Mg (Fig. 3b). Taking actual crown mass (Cm) into account in the biomass allometric model (i.e., m_1) corrected for a similar bias pattern observed when m_0 was fitted to DATA_{CM2} (Fig. 4a). This result shows that variation in crown mass among trees is a major source of bias in the reference biomass allometric model, m_0 .

Using our simulation procedure, we propagated individual prediction errors of m_0 and m_1 to the 130 1 ha field plots from central Africa (Fig. 4b). This process revealed that m_0 led to an average plot-level relative prediction error (S_{plot}) ranging from -23 to $+16\%$ (mean: $+6.8\%$) on PAGB_{pred}, which dropped to $+1$ to $+4\%$ (mean: $+2.6\%$) with m_1 taking crown mass into account.

Because in practice crown mass cannot be routinely measured in the field, we tested the potential of crown mass proxies to improve biomass allometric models. Model m_2 , which used a compound variable integrating crown depth i.e., $(D^2 \times Hc \times \rho)^2$, as a proxy of crown mass outperformed m_0 (Table 2). Although the gain in precision (RSE and S) over m_0 was rather low, the model provided the major advantage of being free of significant local bias towards large trees (> 1 Mg; Fig. 5a). At the plot level, this model provided a much higher precision (0 to 10 % on PAGB_{pred}) and a lower bias (average error of 5 %) than the reference pantropical model m_0 (Fig. 5b). Using a compound variable integrating crown size, i.e., $(D^2 \times Cs \times \rho)^2$, as a crown mass proxy (m_3),

Table 1. Crown mass sub-models. Model variables are Cm (crown mass, kg), *D* (diameter at breast height, cm), Hc (crown depth, m), Cs (average of Hc and crown diameter, m) and ρ (wood density, g cm^{-3}). The general form of the models is $\ln(Y) = a + b \times \ln(X) + c \times \ln(X)^2$. Model coefficient estimates are provided along with the associated standard error, which is denoted by SE_i , with *i* as the coefficient.

Model	Data set	Model input			Model parameters					Model performance					
		<i>Y</i>	<i>X</i>	X^2	<i>a</i>	<i>b</i>	<i>c</i>	SE_a	SE_b	SE_c	R^2	RSE	<i>S</i>	AIC	dF
sm ₁	Data _{CM2} (<i>n</i> = 541)	Cm	$D^2 \times Hc \times \rho$	–	–2.6345 ^a	0.9368 ^a		0.1145	0.0125		0.91	0.615	36.0	1012.6	539
sm ₃			$D^2 \times Hc \times \rho$	$(D^2 \times Hc \times \rho)^2$	0.9017 ^d	0.1143 ^{ns}	0.0452 ^a	0.5049	0.1153	0.0063	0.92	0.588	35.2	965.2	538
			–	$(D^2 \times Hc \times \rho)^2$		1.3990 ^a		0.0514 ^a	0.0605		0.0007	0.92	0.588	35.5	964.2
sm ₁	Data _{CD} (<i>n</i> = 119)	Cm	$D^2 \times Hc \times \rho$	–	–2.9115 ^a	0.9843 ^a		0.3139	0.0289		0.91	0.516	31.8	184.1	117
sm ₂			$D^2 \times Cs \times \rho$	–	–3.0716 ^a	0.9958 ^a		0.2514	0.0231		0.94	0.414	21.8	131.9	117
sm ₃			$D^2 \times Hc \times \rho$	$D^2 \times Hc \times \rho^2$	–0.2682 ^{ns}	0.4272 ^{ns}	0.0283	1.4077	0.2908	0.0147	0.91	0.510	29.7	182.3	116
			–	$D^2 \times Hc \times \rho^2$		1.7830 ^a		0.0498 ^a	0.1774	0.0015	0.91	0.512	32.2	182.5	117
sm ₄			$D^2 \times Cs \times \rho$	$D^2 \times Cs \times \rho^2$	–0.5265 ^{ns}	0.4617	0.0270 ^c	1.1443	0.2356	0.0119	0.94	0.407	128.7	25.9	116
	–	$D^2 \times Cs \times \rho^2$		1.6994 ^a		0.0502 ^a	0.1421		0.0012	0.94	0.412	130.5	25.8	117	

Coefficients' probability value (pv) is coded as follows: ^a $pv \leq 10^{-4}$; ^b $pv \leq 10^{-3}$; ^c $pv \leq 10^{-2}$; ^d $pv \leq 0.05$; "ns" – $pv \geq 0.05$. Models' performance parameters are R^2 (adjusted *R* square), RSE (residual standard error), *S* (median of unsigned relative individual errors, in %), AIC (Akaike information criterion), and dF (degree of freedom).

Table 2. Models used to estimate tree AGB. Model parameters are *D* (diameter at breast height, cm), *H* (total height, m), Ht (trunk height, m), Hc (crown depth, m), Cm (crown mass, kg), Cs (average of Hc and crown diameter, m) and ρ (wood density, g cm^{-3}). The general form of the models is $\ln(Y) = a + b \times \ln(X_1) + c \times \ln(X_2)$. Model coefficient estimates are provided along with the associated standard error is denoted by SE_i , with *i* as the coefficient.

Model	Data set	Model input			Model parameters					Model performance					
		<i>Y</i>	X_1	X_2	<i>a</i>	<i>b</i>	<i>c</i>	SE_a	SE_b	SE_c	R^2	RSE	<i>S</i>	AIC	dF
m ₀	Data _{REF} (<i>n</i> = 4004)	AGB	$D^2 \times H \times \rho$		–2.7628 ^a	0.9759 ^a		0.0211	0.0026		0.97	0.358	22.1	3130.7	4002
m ₀	Data _{CM2} (<i>n</i> = 541)	AGB	$D^2 \times H \times \rho$		–2.5860 ^a	0.9603 ^a		0.0659	0.0066		0.98	0.314	18.9	284.8	539
m ₁			$D^2 \times Ht \times \rho$	Cm	–0.5619 ^a	0.5049 ^a	0.4816 ^a	0.0469	0.0098	0.0096	0.99	0.199	9.8	–205.7	538
m ₂			$D^2 \times Ht \times \rho$	$(D^2 \times Hc \times \rho)^2$	0.3757 ^a	0.4451 ^a	0.0281 ^a	0.0974	0.0186	0.0010	0.98	0.298	17.8	231.5	538
m ₀	Data _{CD} (<i>n</i> = 119)	AGB	$D^2 \times H \times \rho$		–3.1105 ^a	1.0119 ^a		0.1866	0.0160		0.97	0.268	15.0	28.1	117
m ₁			$D^2 \times Ht \times \rho$	Cm	–0.5851 ^a	0.4784 ^a	0.5172 ^a	0.1117	0.0203	0.0185	0.99	0.142	7.0	–121.2	116
m ₂			$D^2 \times Ht \times \rho$	$(D^2 \times Hc \times \rho)^2$	–0.2853 ^{ns}	0.5804 ^a	0.0216 ^a	0.2499	0.0397	0.0019	0.97	0.272	14.5	32.5	116
m ₃			$D^2 \times Ht \times \rho$	$(D^2 \times Cs \times \rho)^2$	0.5800 [*]	0.4263 ^a	0.0283 ^a	0.2662	0.0444	0.0021	0.98	0.246	12.3	9.3	116

Coefficients' probability value (pv) is coded as follows: ^a $pv \leq 10^{-4}$; ^b $pv \leq 10^{-3}$; ^c $pv \leq 10^{-2}$; ^d $pv \leq 0.05$; "ns" – $pv \geq 0.05$. Models' performance parameters are R^2 (adjusted *R* square), RSE (residual standard error), *S* (median of unsigned relative individual errors, in %), AIC (Akaike information criterion), and dF (degree of freedom).

thus requiring both crown depth and diameter measurements, significantly improved model precision (m₃ vs. m₂; Table 2) while preserving the relatively unbiased distribution of relative residuals (results not shown).

4 Discussion

Using a data set of 673 individuals, including most of the largest trees that have been destructively sampled to date, we discovered tremendous variation in the crown mass ratio among tropical trees, ranging from 3 to 88 %, with an average of 36 %. This variation was not independent of tree size, as indicated by a marked increase in the crown mass ratio with tree mass for trees ≥ 10 Mg. This threshold was mirrored by a breaking point in the relationship between total tree mass and the compound predictor variable used in the reference allometric model of Chave et al. (2014). When the compound variable is limited to trunk mass prediction and a crown mass predictor is added to the model, the bias towards large trees is significantly reduced. As a consequence, error propaga-

tion to plot-level AGB estimations is largely reduced. In the following section, we discuss the significance and implication of these findings from both an ecological and a practical point of view with respect to resource allocation to the tree compartments and to carbon storage in forest aboveground biomass.

4.1 Crown mass ratio and the reference biomass model error

We observed an overall systematic increase in the crown mass ratio with tree mass. This ontogenetic trend has already been reported for some tropical canopy species (O'Brien et al., 1995) and likely reflects changes in the pattern of resource allocation underlying crown edification in most forest canopy trees (Barthélémy and Caraglio, 2007; Hasenauer and Monserud, 1996; Holdaway, 1986; Moorby and Wareing, 1963; Perry, 1985). The overall increase in the carbon accumulation rate with tree size is a well-established trend (Stephenson et al., 2014), but the relative contribution of the trunk and the crown to that pattern has rarely been

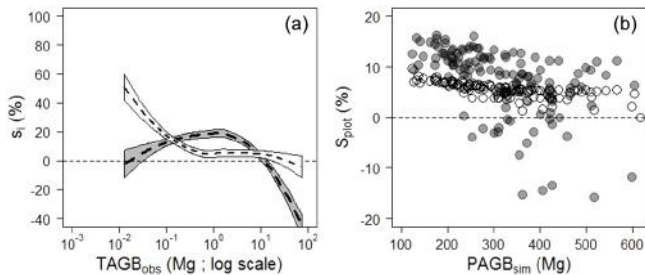


Figure 5. Panel (a): relative individual residuals (s_i , in %) obtained with the reference biomass allometric model m_0 (grey background) and with our model m_2 including a crown mass proxy (white background). Thick dashed lines represent fits of local regressions (loess function; span: 1) bounded by standard errors. Panel (b): propagation of individual residual errors of m_0 (solid grey circles) and m_2 (empty circles) to the plot level.

investigated, particularly for large trees for which branch growth monitoring involves a tremendous amount of work. Sillett et al. (2010) collected a unique data set in this regard, with detailed growth measurements on very old (up to 1850 years) and large (up to 648 cm D) individuals of *Eucalyptus regnans* and *Sequoia sempervirens* species. For these two species, the contribution of crown to AGB growth increased linearly with tree size and thus with the crown mass ratio. We observed the same tendency in our data for trees ≥ 10 Mg (typically with $D > 100$ cm). This result thus suggests that biomass allometric relationships may differ among small and large trees, thus explaining the systematic underestimation of AGB for large trees observed by Chave et al. (2014). These authors suggested that underestimations induced by their model were due to a potential “majestic tree” sampling bias, according to which scientists would have more systematically sampled trees with well-formed boles and healthy crowns. We agree that such an effect cannot be completely ruled out, and it is probably all the more significant that trees ≥ 10 Mg represent only 3 % of the reference data set of Chave et al. (2014). Collecting more field data on large trees should therefore constitute a priority if we are to improve multi-specific, broad-scale allometric models, and the recent development of nondestructive AGB estimation methods based on terrestrial lidar data should help in this regard (e.g., Calders et al., 2015). However, regardless of whether the nonlinear increase in crown mass ratio with tree mass held to a sampling artifact, we have shown that it was the source of systematic error in the reference model that used a unique geometric approximation with an average form factor for all trees. This finding agrees with the results of Goodman et al. (2014) in Peru, who found significant improvements in biomass estimates of large trees when biomass models included tree crown radius, thus partially taking crown ratio variations into account. Identifying predictable patterns of crown mass ratio variation, as performed for crown size allometries specific to some functional groups (Poorter et al.,

2003, 2006; Van Gelder et al., 2006), therefore appears to be a potential way to improve allometric-model performance.

4.2 Model error propagation depends on targeted plot structure

The reference pantropical model provided by Chave et al. (2014) presents a bias pattern that is a function of tree size (i.e., average overestimation of small tree AGB and average underestimation of large tree AGB). Propagation of individual errors to the plot level therefore depends on tree size distribution in the sample plot, with over- or underestimations depending on the relative importance of small or large trees in the stand (e.g., young secondary forests vs. old-growth forests; see Appendix B for more information on the interaction between model error, plot structure and plot size). This effect is not consistent with the general assumption that individual errors should be compensated for at the plot level. Although the dependence of error propagation on tree size distribution has already been raised (Magnabosco Marra et al., 2015; Mascaro et al., 2011), it is generally omitted from error propagation procedures (e.g., Picard et al., 2014; Moundounga Mavouroulou et al., 2014; Chen et al., 2015). When propagating local bias to 130 1 ha plots in central Africa, the reference pantropical model led to plot-level errors ranging from -15 to $+8$ %. The presence of large trees, in particular their relative contribution to stand total AGB, explained most between-plot error variation (Appendix B). We can therefore hypothesize that in the neotropics, where large trees are less common in forests than in the paleotropics (Lewis et al., 2013; Slik et al., 2013), the model would more systematically overestimate plot AGB. Interestingly, most of the plots undergoing a systematic AGB underestimation (i.e., high number of large trees) were located in the Atlantic forests of western Cameroon (Korup National Park), where large individuals of *Lecomtedoxa klaineana* (Pierre ex Engl) – a so-called “biomass hyperdominant” species (sensu Bastin et al., 2015) – are particularly abundant. Interactions between model error and forest structure may thus also hinder the detection of spatial variations in forest AGB between forest types as well as on local scales, e.g., between patches dominated by *Lecomtedoxa klaineana* trees or not. On the landscape or regional scale, plot-level errors may average out if the study area is a mosaic of forests with varying tree size distributions. However, if plot estimations are used to calibrate remote sensing products, individual plot errors may propagate as a systematic bias in the final extrapolation (Réjou-Méchain et al., 2014).

4.3 Taking crown mass variation into account in allometric models

We propose a modeling strategy that decomposes total tree mass into trunk and crown masses. A direct benefit of addressing these two components separately is that it should

reduce the error in trunk mass estimation because the trunk form factor is less variable across species than the whole-tree form factor (Cannell, 1984). We modeled tree crown using a geometric solid whose basal diameter and height were the trunk diameter and crown depth, respectively. Crown volume was thus considered as the volume occupied by branches if they were squeezed onto the main stem (“as if a ring were passed up the stem”, Cannell, 1984). Using a simple linear model to relate crown mass to the geometric approximation (sm_1 , sm_2) led to an underestimation bias that gradually increased with crown mass (Fig. 2b). A similar pattern was observed on all crown mass models based on trunk diameter (Appendix A) and reflected a significant change in the relationship between the two variables with crown size. Consistently, a second-order polynomial model better captured such a nonlinear increase in crown mass with trunk diameter-based proxies and thus provided unbiased crown mass estimates (Fig. 2c). Our results agree with those of Sillett et al. (2010), who showed that ground-based measurements such as trunk diameter do not properly render the high rate of mass accumulation in large trees, notably in tree crowns, and may also explain why the dynamics of forest biomass are inferred differently from top-down (e.g., airborne lidar) or bottom-up views (e.g., field measurement; Réjou-Méchain et al., 2015).

Changes in trunk and crown mass along tree ontogeny are not independent and indeed, both variables appeared tightly correlated in our data set. Including crown mass (or a proxy for this variable) as an additive covariate to the trunk mass proxy may thus raise the debate on collinearity between predictors in biomass allometry models (see Picard et al., 2015; Sileshi, 2014). For instance, models m_1 and m_2 calibrated on $Data_{CM2}$ led to a variance inflation factor (VIF) of 5.4 and 8.8, respectively, which is higher than the range of values commonly considered as critical (2–5; Sileshi, 2014). Nevertheless, we have shown that the inclusion of a separate crown component to the models reduced model residuals (greater precision) and improved their distribution over the AGB gradient (greater accuracy) because it allowed us to capture a general trend in our data set of a relative increase in crown mass proportion with tree mass. Assuming that this phenomenon holds in new sets of tropical trees and that we adequately sampled the correlation structure between crown and trunk masses, the issue of predictor collinearity should therefore not dramatically inflate model prediction errors (Picard et al., 2015).

From a practical point of view, our tree biomass model m_2 , which requires only extra information on trunk height (if total height is already measured) provides a better fit than the reference pantropical model and removes estimation bias on large trees. In scientific forest inventories, total tree height is often measured on a subsample of trees, including most of the largest trees in each plot, to calibrate local allometries between H and D . We believe that measuring the trunk height of those trees does not represent a cumbersome amount of additional effort because trunk height is much more easily measured than total tree height. We thus recommend using model m_2 – at least for the largest trees, i.e., those with $D \geq 100$ cm – and encourage future studies to assess its performance from independent data sets. Including more detailed crown measurements into biomass allometric equations could also become a reasonable option in the near future, provided the development of new technologies, like (mobile) terrestrial lidar scanning, will make it possible to easily extract crown data and gather large-scale data sets.

Data availability

Destructive sampling data set available at <http://dx.doi.org/10.5061/dryad.f2b52>.

Appendix A: Crown mass sub-models

A1 Method

Several tree metrics are expected to scale with crown mass, particularly crown height (Mäkelä and Valentine, 2006), crown diameter (King and Loucks, 1978) and trunk diameter (e.g., Nogueira et al., 2008; Chambers et al., 2001). In this study, we tested whether any of these variables (i.e., trunk diameter, crown height and crown diameter) prevailed over the others in explaining crown mass variations. Power functions were fitted in log-transformed form using ordinary least-squares regression techniques (models sm_{1-X}):

$$\ln(Cm) = \alpha + \beta \times \ln(X) + \varepsilon, \quad (A1)$$

where Cm is the crown mass (in kg); X is the structural variable of interest, namely D for trunk diameter at breast height (in cm), Hc for crown depth (in m), or Cd for crown diameter (in m); α and β are the model coefficients; and is ε the error term assumed to follow a normal distribution.

We also assessed the predictive power of the three structural variables on crown mass while controlling for variations in wood density (ρ , in $g\ cm^{-3}$), leading to models sm_{2-X} :

$$\ln(Cm) = \alpha + \beta \times \ln(X) + \gamma \times \ln(\rho) + \varepsilon, \quad (A2)$$

where γ is the model coefficient of ρ .

Similarly to the cylindrical approximation of a tree trunk, we further established a compound variable for tree crown based on D and Hc , leading to model sm_3 :

$$\ln(Cm) = \alpha + \beta \times \ln(D^2 \times Hc \times \rho) + \varepsilon, \quad (A3)$$

where crown height is a proxy for the length of the branching network. Results obtained using sm_3 are presented in the manuscript as well as in this appendix for comparison with those obtained using sm_{1-X} and sm_{2-X} .

A2 Results and discussion

Among the three structural variables tested as proxies for crown mass, trunk diameter provided the best results. Model sm_{1-D} presented a high R^2 (0.88), but its precision was low, with an S (i.e., the median of unsigned s_i values) of 43 % (Table A1). Moreover, model error increased appreciably with crown mass (Fig. A1a). For instance, model estimations for an observed crown mass of approximately 20 Mg ranged between 5 and 55 Mg. Nevertheless, sm_{1-D} outperformed sm_{1-Hc} (Data_{CM2}; AIC of 1182 vs. 1603, respectively) and was slightly better than sm_{1-Cd} (Data_{CD}; AIC of 257 vs. 263, respectively), suggesting that the width of the first branching network pipe is a stronger constraint on branch mass than the external dimensions of the network (i.e., Hc , Cd).

The model based on crown depth (sm_{1-Hc}) was subjected to a large error (S of ca. 80 %; Table A1) and clearly saturated for a crown mass ≥ 10 Mg (Fig. A1b). Because crown

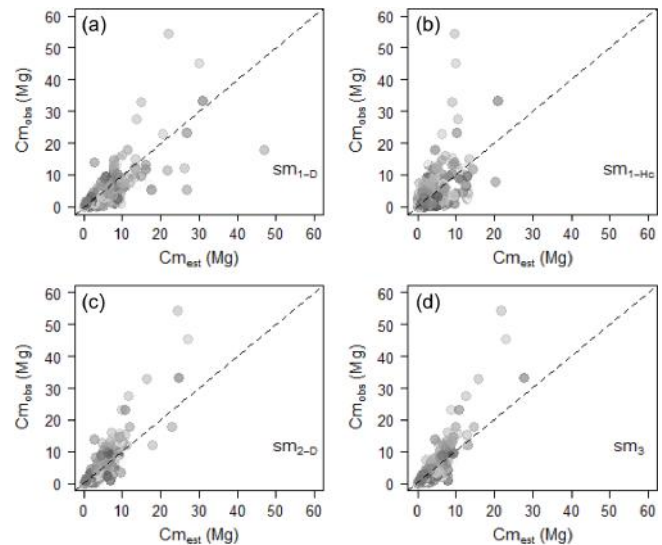


Figure A1. Observed against estimated crown mass (in Mg) for models sm_{1-D} (a), sm_{1-Hc} (b), sm_{2-D} (c), sm_3 (d). Models were calibrated on Data_{CM2}. Tree wood density was standardized to range between 0 and 1 and represented as a greyscale (with black the lowest values and white the highest values).

depth does not take branch angle into account, it does not properly render the length of the branching network. The saturation threshold observed on large crowns supports the observations of Sillett et al. (2010): tree height, from which crown depth directly derives, levels off in large or adult trees, but mass accumulation – notably within the crowns – continues far beyond this point. It follows that crown depth alone does not allow for the detection of the highest mass levels in large or old tree crowns.

The model based on crown diameter presented a weaker fit than sm_{1-D} , with a higher AIC (Data_{CD}, 263 vs. 257) and an individual relative error approximately 10 % higher (S of approximately 50 and 40 %; Table A1). However, crown diameter appeared more informative regarding the mass of the largest crowns than trunk diameter (Fig. A2a and b). In fact, the individual relative error of sm_{1-Cd} on crowns ≥ 10 Mg was only 26 % vs. 47 % for sm_{1-D} .

Taking variations in wood density into account improved the model based on trunk diameter. As shown in Fig. A1, using a color code for wood density highlighted a predictable error pattern in model estimations: trunk diameter tends to over- or underestimate the crown mass of trees with high or low wood density, respectively. This pattern is corrected for in sm_{2-D} , which presents a lower AIC than sm_{1-D} (i.e., 1079) and an individual relative error approximately 15 % lower (i.e., 37 %; Table A1). Interestingly, whereas sm_{2-D} appeared to be more accurate than sm_{1-D} in its estimations of large crown mass (Fig. A1c), it also presented an underestimation bias that gradually increased with crown mass. Including ρ in the model based on Cd improved the model fit (AIC of 251

Table A1. Preliminary crown mass sub-models. Model parameters are D (diameter at breast height, cm), H_c (crown depth, m), C_m (crown mass, kg), C_d (crown diameter, in m), C_s (average of H_c and C_d , m) and ρ (wood density, g cm^{-3}). The general form of the models is $\ln(Y) = a + b \times \ln(X_1) + c \times \ln(X_2)$. Model coefficient estimates are provided along with the associated standard error is denoted by SE_i , with i as the coefficient.

Model	Data set	Model input			Model parameters						Model performance				
		Y	X_1	X_2	a	b	c	SE_a	SE_b	SE_c	R^2	RSE	S	AIC	dF
1-D	Data _{CM2} ($n = 541$)	C_m	D		-3.6163 ^a	2.5786 ^a		0.1514	0.0409		0.88	0.719	42.8	1181.6	539
1-Hc			H_c		-0.1711 ^{ns}	2.6387 ^a		0.1574	0.0673		0.74	1.060	82.2	1602.8	539
2-D			D	ρ	-3.0876 ^a	2.6048 ^a	1.1202 ^a	0.1462	0.0372	0.1048	0.90	0.653	36.7	1079.4	538
2-Hc			H_c	ρ	-0.3952 ^c	2.6574 ^a	-0.3274 ^d	0.1959	0.0679	0.1712	0.74	1.058	80.6	1601.1	538
3				$D^2 \times H_c \times \rho$	-2.6345 ^a	0.9368 ^a		0.1145	0.0125		0.91	0.615	36.0	1012.6	539
1-D	Data _{CD} ($n = 119$)	C_m	D		-3.4603 ^a	2.5684 ^a		0.4692	0.1075		0.83	0.702	39.8	257.4	117
1-Hc			H_c		1.3923 ^c	2.2907 ^a		0.5392	0.1938		0.54	1.149	77.4	374.7	117
1-Cd			C_d		-0.1181 ^{ns}	2.8298 ^a		0.3403	0.1218		0.82	0.718	52.7	262.8	117
2-D			D	ρ	-2.7296 ^a	2.6293 ^a	1.5243 ^a	0.3528	0.0793	0.1523	0.91	0.516	30.5	185.3	116
2-Hc			H_c	ρ	1.1181 ^{ns}	2.3356 ^a	-0.2326 ^{ns}	0.6869	0.2063	0.3596	0.54	1.152	82.9	376.3	116
2-Cd			C_d	ρ	0.4677 ^{ns}	2.7954 ^a	0.7538 ^a	0.3585	0.1158	0.2009	0.84	0.681	44.5	251.2	116

Coefficients' probability value (pv) is coded as follows: ^a $pv \leq 10^{-4}$; ^b $pv \leq 10^{-3}$; ^c $pv \leq 10^{-2}$; ^d $pv \leq 0.05$; "ns" - $pv \geq 0.05$. Models' performance parameters are R^2 (adjusted R square), RSE (residual standard error), S (median of unsigned relative individual errors, in %), AIC (Akaike information criterion), and dF (degree of freedom).

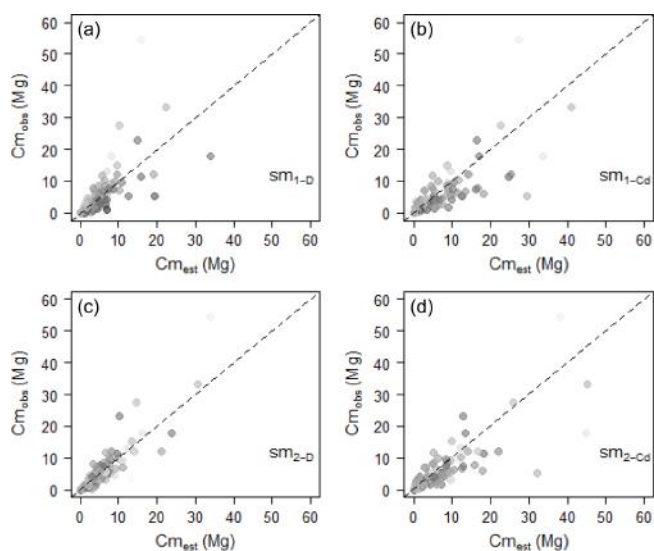


Figure A2. Observed vs. estimated crown mass (in Mg) for models sm_{1-D} (a), sm_{1-Cd} (b), sm_{2-D} (c), sm_{2-Cd} (d). Models were calibrated on Data_{CD}. Tree wood density was standardized to range between 0 and 1 and is represented as a greyscale (with black the lowest values and white the highest values).

vs. 262 for sm_{2-Cd} and sm_{1-Cd} , respectively) and decreased the individual relative error by approximately 15%. Similarly to sm_{1-Cd} , sm_{2-Cd} was outperformed by its counterpart based on D (AIC of 185). Moreover, the gain in precision in sm_{2-Cd} was localized on small crowns, whereas estimations regarding large crowns were fairly equivalent (Fig. A2c–d). Model 2-D was more precise regarding crowns ≥ 10 Mg, with an individual relative error of 23% vs. 32% for sm_{2-Cd} .

The strongest crown mass predictor, D , was used as the basis of a geometric solid approximating crown volume ($D^2 \times H_c$) and, in turn, mass ($D^2 \times H_c \times \rho$) in model sm_3 . With one less parameter than sm_{2-D} , sm_3 presented a lower AIC (i.e., 1012), but the two models provided a fairly similar fit to the observations (RSE of 0.65 vs. 0.61 and S of 37% vs. 36% for sm_{2-D} and sm_3 , respectively). This result indicates that when D and ρ are known, information on crown depth is of minor importance for predicting crown mass. However, this conclusion applies to our data set only because H_c might be more informative regarding crown mass variations when considering sites or species with more highly contrasting $D - H$ or $D - H_c$ relationships.

Similarly to sm_{2-D} , sm_3 presented an underestimation bias that increased gradually with crown mass (illustrated in Fig. A1d).

Appendix B: Plot-level error propagation

We used the error propagation procedure described in the “Methods” section of the manuscript to estimate the mean plot-level AGB prediction error that could be expected from m_0 calibrated on $DATA_{REF}$ (i.e., the pantropical model proposed in Chave et al., 2014). Model error was propagated on 80 1 ha sample plots of tropical forest in central Africa (field inventory protocol in Supplement Sect. S1.3), to which we added 50 1 ha plots from the Korup 50 ha permanent plot (Chuyong et al., 2004). We further subsampled the Korup 50 ha permanent plot in subplots of varying sizes (from 25 to 0.1 ha) to evaluate the effect of plot size on plot-level AGB prediction error.

From the simulated $PAGB_{sim}$ for the 130 1 ha plots, we estimated that the reference pantropical model, m_0 , propagated to $PAGB_{pred}$ a mean prediction error (over 1000 realizations of S_{plot}) that ranged between -15 and $+7.7\%$ (Fig. B1a), mostly caused by trees with mass ≥ 20 Mg (Fig. B1b). This trend was particularly evident in the undisturbed evergreen stands of Korup (triangles in Fig. B1a–b), where patches of *Lecomtedoxa klaineana* (Pierre ex Engl) individuals largely drove the $PAGB_{pred}$ predictions ($R^2 = 0.87$, model II ordinary least squares regression method). This species generates high-statured individuals of high wood density, which frequently exceed 20 Mg and result in underestimates of plot-level biomass. Interestingly, some high-biomass plots could still be overestimated when $PAGB_{pred}$ was concentrated in trees weighing less than 20 Mg.

As a consequence of m_0 bias concentration in large trees, plot-level prediction errors for the 50 ha in Korup tended to stabilize near 0 for subplots ≥ 5 ha only. Below this threshold (i.e., for subplots ≤ 1 ha), the median error is positive but negative outliers are more frequent (Fig. B2). Indeed, on the one hand, small plots are less likely to include large trees and have a positive prediction error of up to approximately $+7.5\%$. On the other hand, a single large tree can strongly affect $PAGB_{pred}$, occasionally leading to a large underestimation of small plots AGB that can exceed -15% for a 0.25 ha and -20% for a 0.1 ha subplot.

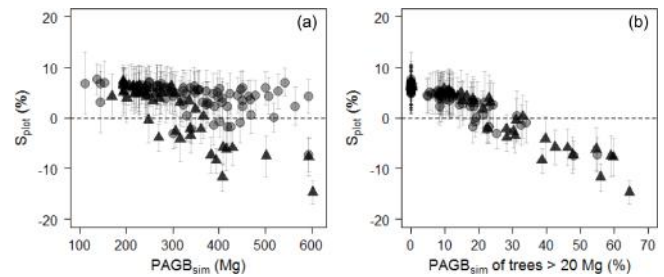


Figure B1. Plot-level propagation of individual-level model error. Panel (a): mean relative error (S_{plot} , in %) and standard deviation of 1000 random error sampling against simulated plot AGB and (b) against the fraction (%) of simulated plot AGB accounted for by trees > 20 Mg. Plots from the Korup permanent plot are represented by triangles.

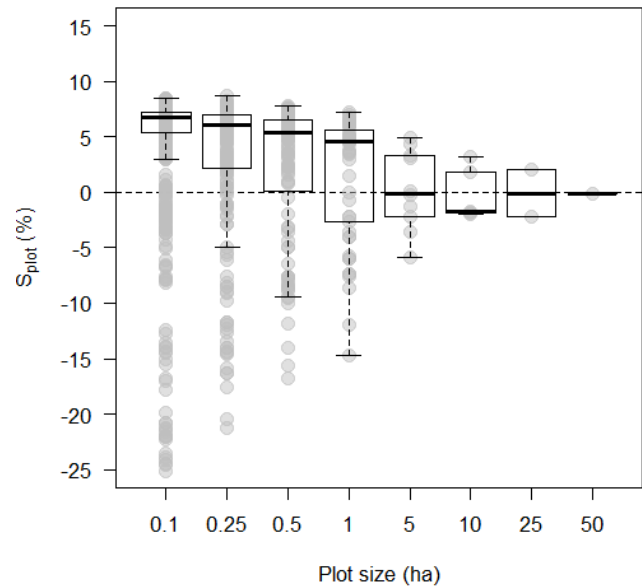


Figure B2. Plot-level relative error (S_{plot} , in %) as a function of plot size (in ha) in the Korup permanent plot. Individual plot values are represented by grey dots.

The Supplement related to this article is available online at doi:10.5194/bg-13-1571-2016-supplement.

Author contributions. Conception and design of the experiments: Pierre Ploton, Nicolas Barbier and Raphaël Pélissier. Data collection (unpublished destructive data and field inventories): Stéphane Takoudjou Momo, Bonaventure Sonké, Narcisse Guy Kamdem, Moses Libalah, Donatien Zebaze, Nicolas Texier, Faustin Boyemba Bosela, John Katembo Mukirania, Gilles Dauby, Vincent Droissart. Data sharing: Georges Chuyong, David Kenfack, Duncan Thomas, Adeline Fayolle, Alfred Ngomanda, Matieu Henry, Rosa Calisto Goodman. Analysis of the data: Pierre Ploton. Analysis feedback: Raphaël Pélissier, Nicolas Barbier, Vivien Rossi, Maxime Réjou-Méchain, Uta Berger. Writing of the paper: Pierre Ploton, Raphaël Pélissier and Maxime Réjou-Méchain. Writing feedback: Nicolas Barbier, Adeline Fayolle, Vivien Rossi, Pierre Couteron, Matieu Henry, Rosa Calisto Goodman.

Acknowledgements. Destructive data from Cameroon were collected with the financial support from the IRD project PPR FTH-AC “Changements globaux, biodiversité et santé en zone forestière d’Afrique Centrale” and the support and involvement of the Alpicam Company. A portion of the plot data were collected with the support of the CoForTips project as part of the ERA-Net BiodivERsA 2011–2012 European joint call (ANR-12-EBID-0002). Pierre Ploton was supported by an Erasmus Mundus PhD grant from the 2013–2016 Forest, Nature and Society (FONASO) doctoral program.

Edited by:

References

- Avitabile, V., Herold, M., Henry, M., and Schimullius, C.: Mapping biomass with remote sensing: a comparison of methods for the case study of Uganda, *Carbon Balance and Management*, 6, 1–14, 2011.
- Baccini, A., Goetz, S. J., Walker, W. S., Laporte, N. T., Sun, M., Sulla-Menashe, D., Hackler, J., Beck, P. S. A., Dubayah, R., and Friedl, M. A.: Estimated carbon dioxide emissions from tropical deforestation improved by carbon-density maps, *Nature Climate Change*, 2, 182–185, 2012.
- Barthélémy, D. and Caraglio, Y.: Plant Architecture: A Dynamic, Multilevel and Comprehensive Approach to Plant Form, Structure and Ontogeny, *Ann. Bot.*, 99, 375–407, doi:10.1093/aob/mcl260, 2007.
- Baskerville, G. L.: Use of Logarithmic Regression in the Estimation of Plant Biomass, *Can. J. Forest Res.*, 2, 49–53, doi:10.1139/x72-009, 1972.
- Bastin, J.-F., Barbier, N., Réjou-Méchain, M., Fayolle, A., Gourlet-Fleury, S., Maniatis, D., de Haulleville, T., Baya, F., Beeckman, H., and Beina, D.: Seeing Central African forests through their largest trees, *Scientific Reports*, 5, 13156, doi:10.1038/srep13156, 2015.
- Beygelzimer, A., Kakadet, S., Langford, J., Arya, S., Mount, D., and Li, S.: FNN: fast nearest neighbor search algorithms and applications, R package version 1.1., 2013.
- Brown, S., Gillespie, A. J., and Lugo, A. E.: Biomass estimation methods for tropical forests with applications to forest inventory data, *For. Sci.*, 35, 881–902, 1989.
- Calders, K., Newnham, G., Burt, A., Murphy, S., Raunonen, P., Herold, M., Culvenor, D., Avitabile, V., Disney, M., Armston, J., and Kaasalainen, M.: Nondestructive estimates of above-ground biomass using terrestrial laser scanning, edited by: McMahon, S., *Methods in Ecology and Evolution*, 6, 198–208, doi:10.1111/2041-210X.12301, 2015.
- Cannell, M. G. R.: Woody biomass of forest stands, *Forest Ecol. Manag.*, 8, 299–312, doi:10.1016/0378-1127(84)90062-8, 1984.
- Chambers, J. Q., dos Santos, J., Ribeiro, R. J., and Higuchi, N.: Tree damage, allometric relationships, and above-ground net primary production in central Amazon forest, *Forest Ecol. Manag.*, 152, 73–84, 2001.
- Chave, J., Andalo, C., Brown, S., Cairns, M. A., Chambers, J. Q., Eamus, D., Fölster, H., Fromard, F., Higuchi, N., Kira, T., Lescure, J.-P., Nelson, B. W., Ogawa, H., Puig, H., Riéra, B., and Yamakura, T.: Tree allometry and improved estimation of carbon stocks and balance in tropical forests, *Oecologia*, 145, 87–99, doi:10.1007/s00442-005-0100-x, 2005.
- Chave, J., Coomes, D., Jansen, S., Lewis, S. L., Swenson, N. G., and Zanne, A. E.: Towards a worldwide wood economics spectrum, *Ecol. Lett.*, 12, 351–366, doi:10.1111/j.1461-0248.2009.01285.x, 2009.
- Chave, J., Réjou-Méchain, M., Búrquez, A., Chidumayo, E., Colgan, M. S., Delitti, W. B. C., Duque, A., Eid, T., Fearnside, P. M., Goodman, R. C., Henry, M., Martínez-Yrizar, A., Mugasha, W. A., Muller-Landau, H. C., Mencuccini, M., Nelson, B. W., Ngomanda, A., Nogueira, E. M., Ortiz-Malavassi, E., Pélissier, R., Ploton, P., Ryan, C. M., Saldarriaga, J. G., and Vieilledent, G.: Improved allometric models to estimate the aboveground biomass of tropical trees, *Glob. Change Biol.*, 20, 3177–3190, doi:10.1111/gcb.12629, 2014.
- Chen, Q., Vaglio Laurin, G., and Valentini, R.: Uncertainty of remotely sensed aboveground biomass over an African tropical forest: Propagating errors from trees to plots to pixels, *Remote Sens. Environ.*, 160, 134–143, doi:10.1016/j.rse.2015.01.009, 2015.
- Chuyong, G. B., Condit, R., Kenfack, D., Losos, E., Sainge, M., Songwe, N. C., and Thomas, D. W.: Korup forest dynamics plot, Cameroon, in: *Forest diversity and dynamism: findings from a large-scale plot network*, edited by: Losos, E. C. and Leigh Jr., E. G., University of Chicago Press, Chicago, 506–516, 2004.
- Clark, D. B. and Clark, D. A.: Abundance, growth and mortality of very large trees in neotropical lowland rain forest, *Forest Ecol. Manag.*, 80, 235–244, doi:10.1016/0378-1127(95)03607-5, 1996.
- Clark, D. B. and Kellner, J. R.: Tropical forest biomass estimation and the fallacy of misplaced concreteness, *J. Veg. Sci.*, 23, 1191–1196, doi:10.1111/j.1654-1103.2012.01471.x, 2012.
- Cleveland, W. S., Grosse, E., and Shyu, W. M.: Local regression models, *Stat. Model.*, 8, 309–376, 1992.
- Eggleston, H. S., Buendia, L., Miwa, K., Ngara, T., and Tanabe, K.: IPCC guidelines for national greenhouse gas inventories, *Inst. Glob. Environ. Strateg. Hayama Jpn.*, 2006.

- Eloy, C.: Leonardo's rule, self-similarity and wind-induced stresses in trees, *Phys. Rev. Lett.*, 107, 258101, doi:10.1103/PhysRevLett.107.258101, 2011.
- Enquist, B. J.: Universal scaling in tree and vascular plant allometry: toward a general quantitative theory linking plant form and function from cells to ecosystems, *Tree Physiol.*, 22, 1045–1064, doi:10.1093/treephys/22.15-16.1045, 2002.
- Fayolle, A., Doucet, J.-L., Gillet, J.-F., Bourland, N., and Lejeune, P.: Tree allometry in Central Africa: Testing the validity of pantropical multi-species allometric equations for estimating biomass and carbon stocks, *Forest Ecol. Manag.*, 305, 29–37, doi:10.1016/j.foreco.2013.05.036, 2013.
- Freedman, B., Duinker, P. N., Barclay, H., Morash, R., and Prager, U.: Forest biomass and nutrient studies in central Nova Scotia, *Inf. Rep. Marit. For. Res. Cent. Can.*, (M-X-134), 126 pp., 1982.
- Goodman, R. C., Phillips, O. L., and Baker, T. R.: Data from: The importance of crown dimensions to improve tropical tree biomass estimates, available at: <http://dx.doi.org/10.5061/dryad.p281g> (last access: 17 May 2015), 2013.
- Goodman, R. C., Phillips, O. L., and Baker, T. R.: The importance of crown dimensions to improve tropical tree biomass estimates, *Ecol. Appl.*, 24, 680–698, 2014.
- Hansen, M. C., Potapov, P. V., Moore, R., Hancher, M., Turubanova, S. A., Tyukavina, A., Thau, D., Stehman, S. V., Goetz, S. J., and Loveland, T. R.: High-resolution global maps of 21st-century forest cover change, *Science*, 342, 850–853, 2013.
- Harris, N. L., Brown, S., Hagen, S. C., Saatchi, S. S., Petrova, S., Salas, W., Hansen, M. C., Potapov, P. V., and Lutsch, A.: Baseline map of carbon emissions from deforestation in tropical regions, *Science*, 336, 1573–1576, 2012.
- Hasenauer, H. and Monserud, R. A.: A crown ratio model for Austrian forests, *Forest Ecol. Manag.*, 84, 49–60, doi:10.1016/0378-1127(96)03768-1, 1996.
- Henry, M., Besnard, A., Asante, W. A., Eshun, J., Adu-Bredu, S., Valentini, R., Bernoux, M., and Saint-André, L.: Wood density, phytomass variations within and among trees, and allometric equations in a tropical rainforest of Africa, *Forest Ecol. Manag.*, 260, 1375–1388, doi:10.1016/j.foreco.2010.07.040, 2010.
- Holdaway, M. R.: Modelling Tree Crown Ratio, *Forest Chron.*, 62, 451–455, doi:10.5558/ffc62451-5, 1986.
- Jenkins, J. C., Chojnacky, D. C., Heath, L. S., and Birdsey, R. A.: National-Scale Biomass Estimators for United States Tree Species, *For. Sci.*, 49, 12–35, 2003.
- King, D. and Loucks, O. L.: The theory of tree bole and branch form, *Radiat. Environ. Bioph.*, 15, 141–165, doi:10.1007/BF01323263, 1978.
- Legendre, P.: *lmodel2: Model II Regression*. R package version 1.7-0, See [Httpcran R-Project, Orgwebpackageslmodel2](http://cran.R-Project.org/web/packages/lmodel2), 2011.
- Lewis, S. L., Sonke, B., Sunderland, T., Begne, S. K., Lopez-Gonzalez, G., van der Heijden, G. M. F., Phillips, O. L., Affum-Baffoe, K., Baker, T. R., Banin, L., Bastin, J.-F., Beekman, H., Boeckx, P., Bogaert, J., De Canniere, C., Chezeaux, E., Clark, C. J., Collins, M., Djagbletey, G., Djuikouo, M. N. K., Droissart, V., Doucet, J.-L., Ewango, C. E. N., Fauset, S., Feldpausch, T. R., Foli, E. G., Gillet, J.-F., Hamilton, A. C., Harris, D. J., Hart, T. B., de Haulleville, T., Hladik, A., Hufkens, K., Huygens, D., Jeanmart, P., Jeffery, K. J., Kearsley, E., Leal, M. E., Lloyd, J., Lovett, J. C., Makana, J.-R., Malhi, Y., Marshall, A. R., Ojo, L., Peh, K. S.-H., Pickavance, G., Poulsen, J. R., Reitsma, J. M., Sheil, D., Simo, M., Steppe, K., Taedoumg, H. E., Talbot, J., Taplin, J. R. D., Taylor, D., Thomas, S. C., Toirambe, B., Verbeeck, H., Vleminckx, J., White, L. J. T., Willcock, S., Woell, H., and Zemagho, L.: Above-ground biomass and structure of 260 African tropical forests, *Philos. T. R. Soc. B*, 368, 20120295–20120295, doi:10.1098/rstb.2012.0295, 2013.
- Magnabosco Marra, D., Higuchi, N., Trumbore, S. E., Ribeiro, G. H. P. M., dos Santos, J., Carneiro, V. M. C., Lima, A. J. N., Chambers, J. Q., Negrón-Juárez, R. I., Holzwarth, F., Reu, B., and Wirth, C.: Predicting biomass of hyperdiverse and structurally complex Central Amazon forests – a virtual approach using extensive field data, *Biogeosciences Discuss.*, accepted, 12, 15537–15581, doi:10.5194/bgd-12-15537-2015, 2015.
- Mäkelä, A. and Valentine, H. T.: Crown ratio influences allometric scaling of trees, *Ecology*, 87, 2967–2972, doi:10.1890/0012-9658(2006)87[2967:CRIASI]2.0.CO;2, 2006.
- Malhi, Y., Wood, D., Baker, T. R., Wright, J., Phillips, O. L., Cochrane, T., Meir, P., Chave, J., Almeida, S., and Arroyo, L.: The regional variation of aboveground live biomass in old-growth Amazonian forests, *Glob. Change Biol.*, 12, 1107–1138, 2006.
- Mascaro, J., Litton, C. M., Hughes, R. F., Uowolo, A., and Schnitzer, S. A.: Minimizing Bias in Biomass Allometry: Model Selection and Log-Transformation of Data, *Biotropica*, 43, 649–653, doi:10.1111/j.1744-7429.2011.00798.x, 2011.
- McMahon, T. A. and Kronauer, R. E.: Tree structures: deducing the principle of mechanical design, *J. Theor. Biol.*, 59, 443–466, 1976.
- Mitchard, E. T., Saatchi, S. S., Baccini, A., Asner, G. P., Goetz, S. J., Harris, N. L., and Brown, S.: Uncertainty in the spatial distribution of tropical forest biomass: a comparison of pan-tropical maps, *Carbon Balance Manag.*, 8, 10, doi:10.1186/1750-0680-8-10, 2013.
- Moorby, J. and Wareing, P. F.: Ageing in Woody Plants, *Ann. Bot.*, 27, 291–308, 1963.
- Moundounga Mavouroulou, Q., Ngomanda, A., Engone Obiang, N. L., Lebamba, J., Gomat, H., Mankou, G. S., Loumeto, J., Mido Iponga, D., Kossi Ditsouga, F., Zinga Koumba, R., Botsika Bobé, K. H., Lépengué, N., Mbatchi, B., and Picard, N.: How to improve allometric equations to estimate forest biomass stocks? Some hints from a central African forest, *Can. J. Forest Res.*, 44, 685–691, doi:10.1139/cjfr-2013-0520, 2014.
- Muggeo, V. M. R.: Estimating regression models with unknown break-points, *Stat. Med.*, 22, 3055–3071, doi:10.1002/sim.1545, 2003.
- Ngomanda, A., Engone Obiang, N. L., Lebamba, J., Moundounga Mavouroulou, Q., Gomat, H., Mankou, G. S., Loumeto, J., Mido Iponga, D., Kossi Ditsouga, F., Zinga Koumba, R., Botsika Bobé, K. H., Mikala Okouyi, C., Nyangadouma, R., Lépengué, N., Mbatchi, B., and Picard, N.: Site-specific vs. pantropical allometric equations: Which option to estimate the biomass of a moist central African forest?, *Forest Ecol. Manag.*, 312, 1–9, doi:10.1016/j.foreco.2013.10.029, 2014.
- Niklas, K. J.: Size-dependent Allometry of Tree Height, Diameter and Trunk-taper, *Ann. Bot.*, 75, 217–227, doi:10.1006/anbo.1995.1015, 1995.
- Nogueira, E. M., Fearnside, P. M., Nelson, B. W., Barbosa, R. I., and Keizer, E. W. H.: Estimates of forest biomass in the Brazilian Amazon: New allometric equations and adjustments to biomass

- from wood-volume inventories, *Forest Ecol. Manag.*, 256, 1853–1867, 2008.
- O'Brien, S. T., Hubbell, S. P., Spiro, P., Condit, R., and Foster, R. B.: Diameter, Height, Crown, and Age Relationship in Eight Neotropical Tree Species, *Ecology*, 76, 1926–1939, doi:10.2307/1940724, 1995.
- Pelletier, J., Ramankutty, N., and Potvin, C.: Diagnosing the uncertainty and detectability of emission reductions for REDD + under current capabilities: an example for Panama, *Environ. Res. Lett.*, 6, 024005, doi:10.1088/1748-9326/6/2/024005, 2011.
- Perry, D. A.: The competition process in forest stands, *Attrib. Trees Crop Plants*, 481–506, 1985.
- Picard, N., Bosela, F. B., and Rossi, V.: Reducing the error in biomass estimates strongly depends on model selection, *Ann. For. Sci.*, 72, 811–923, doi:10.1007/s13595-014-0434-9, 2014.
- Picard, N., Rutishauser, E., Ploton, P., Ngomanda, A., and Henry, M.: Should tree biomass allometry be restricted to power models?, *Forest Ecol. Manag.*, 353, 156–163, doi:10.1016/j.foreco.2015.05.035, 2015.
- Poorter, L., Bongers, F., Sterck, F. J., and Wöll, H.: Architecture of 53 rain forest tree species differing in adult stature and shade tolerance, *Ecology*, 84, 602–608, doi:10.1890/0012-9658(2003)084[0602:AORFTS]2.0.CO;2, 2003.
- Poorter, L., Bongers, L., and Bongers, F.: Architecture of 54 moist-forest tree species: traits, trade-offs, and functional groups, *Ecology*, 87, 1289–1301, doi:10.1890/0012-9658(2006)87[1289:AOMTST]2.0.CO;2, 2006.
- R Core Team: R: A language and environment for statistical computing, R Foundation for Statistical Computing, Vienna, Austria, available at: <http://www.R-project.org/> (last access: January 2013), 2012.
- Réjou-Méchain, M., Muller-Landau, H. C., Detto, M., Thomas, S. C., Le Toan, T., Saatchi, S. S., Barreto-Silva, J. S., Bourg, N. A., Bunyavejchewin, S., Butt, N., Brockelman, W. Y., Cao, M., Cárdenas, D., Chiang, J.-M., Chuyong, G. B., Clay, K., Condit, R., Dattaraja, H. S., Davies, S. J., Duque, A., Esufali, S., Ewango, C., Fernando, R. H. S., Fletcher, C. D., Gunatilleke, I. A. U. N., Hao, Z., Harms, K. E., Hart, T. B., Hérault, B., Howe, R. W., Hubbell, S. P., Johnson, D. J., Kenfack, D., Larson, A. J., Lin, L., Lin, Y., Lutz, J. A., Makana, J.-R., Malhi, Y., Marthews, T. R., McEwan, R. W., McMahon, S. M., McShea, W. J., Muscarella, R., Nathalang, A., Noor, N. S. M., Nytych, C. J., Oliveira, A. A., Phillips, R. P., Pongpattananurak, N., Puchi-Manage, R., Salim, R., Schurman, J., Sukumar, R., Suresh, H. S., Suwanvecho, U., Thomas, D. W., Thompson, J., Uriarte, M., Valencia, R., Vicentini, A., Wolf, A. T., Yap, S., Yuan, Z., Zartman, C. E., Zimmerman, J. K., and Chave, J.: Local spatial structure of forest biomass and its consequences for remote sensing of carbon stocks, *Biogeosciences*, 11, 6827–6840, doi:10.5194/bg-11-6827-2014, 2014.
- Réjou-Méchain, M., Tymen, B., Blanc, L., Fauset, S., Feldpausch, T. R., Monteagudo, A., Phillips, O. L., Richard, H., and Chave, J.: Using repeated small-footprint LiDAR acquisitions to infer spatial and temporal variations of a high-biomass Neotropical forest, *Remote Sens. Environ.*, 169, 93–101, 2015.
- Saatchi, S. S., Harris, N. L., Brown, S., Lefsky, M., Mitchard, E. T., Salas, W., Zutta, B. R., Buermann, W., Lewis, S. L., and Hagen, S.: Benchmark map of forest carbon stocks in tropical regions across three continents, *P. Natl. Acad. Sci. USA*, 108, 9899–9904, 2011.
- Scrucca, L.: Model-based SIR for dimension reduction, *Comput. Stat. Data An.*, 55, 3010–3026, 2011.
- Shinozaki, K., Yoda, K., Hozumi, K., and Kira, T.: A quantitative analysis of plant form—the pipe model theory: I. Basic analyses, 14, 97–105, 1964.
- Sileshi, G. W.: A critical review of forest biomass estimation models, common mistakes and corrective measures, *Forest Ecol. Manag.*, 329, 237–254, doi:10.1016/j.foreco.2014.06.026, 2014.
- Sillett, S. C., Van Pelt, R., Koch, G. W., Ambrose, A. R., Carroll, A. L., Antoine, M. E., and Mifsud, B. M.: Increasing wood production through old age in tall trees, *Forest Ecol. Manag.*, 259, 976–994, doi:10.1016/j.foreco.2009.12.003, 2010.
- Sist, P., Mazzei, L., Blanc, L., and Rutishauser, E.: Large trees as key elements of carbon storage and dynamics after selective logging in the Eastern Amazon, *Forest Ecol. Manag.*, 318, 103–109, doi:10.1016/j.foreco.2014.01.005, 2014.
- Slik, J. W., Paoli, G., McGuire, K., Amaral, I., Barroso, J., Bastian, M., Blanc, L., Bongers, F., Boundja, P., and Clark, C.: Large trees drive forest aboveground biomass variation in moist lowland forests across the tropics, *Global Ecol. Biogeogr.*, 22, 1261–1271, 2013.
- Stephenson, N. L., Das, A. J., Condit, R., Russo, S. E., Baker, P. J., Beckman, N. G., Coomes, D. A., Lines, E. R., Morris, W. K., Rüger, N., Álvarez, E., Blundo, C., Bunyavejchewin, S., Chuyong, G., Davies, S. J., Duque, Á., Ewango, C. N., Flores, O., Franklin, J. F., Grau, H. R., Hao, Z., Harmon, M. E., Hubbell, S. P., Kenfack, D., Lin, Y., Makana, J.-R., Malizia, A., Malizia, L. R., Pabst, R. J., Pongpattananurak, N., Su, S.-H., Sun, I.-F., Tan, S., Thomas, D., van Mantgem, P. J., Wang, X., Wisser, S. K., and Zavala, M. A.: Rate of tree carbon accumulation increases continuously with tree size, *Nature*, 507, 90–93, doi:10.1038/nature12914, 2014.
- Van Gelder, H. A., Poorter, L., and Sterck, F. J.: Wood mechanics, allometry, and life-history variation in a tropical rain forest tree community, *New Phytol.*, 171, 367–378, doi:10.1111/j.1469-8137.2006.01757.x, 2006.
- Vieilledent, G., Vaudry, R., Andriamanohisoa, S. F. D., Rakotonarivo, O. S., Randrianasolo, H. Z., Razafindrabe, H. N., Rakotoarivony, C. B., Ebeling, J., and Rasamoelina, M.: A universal approach to estimate biomass and carbon stock in tropical forests using generic allometric models, *Ecol. Appl.*, 22, 572–583, doi:10.1890/11-0039.1, 2011.
- West, G. B., Brown, J. H., and Enquist, B. J.: A general model for the structure and allometry of plant vascular systems, *Nature*, 400, 664–667, doi:10.1038/23251, 1999.
- Zanne, A. E., Lopez-Gonzalez, G., Coomes, D. A., Ilic, J., Jansen, S., Lewis, S. L., Miller, R. B., Swenson, N. G., Wiemann, M. C., and Chave, J.: Data from: towards a worldwide wood economics spectrum, Dryad Digital Reposit, 2009.